

3D CYCLIC FRACTURE ANALYSIS OF BEAM-COLUMN CONNECTIONS

J. Ozbolt, Y.-J. Li, and R. Eligehausen,
Institut für Werkstoffe im Bauwesen, University of Stuttgart,
Germany

Abstract

In recent years significant effort in modeling of concrete and RC structures loaded under general conditions has been made. At the macroscopical level of the material modeling the main difficulty appears to be modeling of concrete. The microplane model for concrete has been recently improved and extended for general use in 3D fracture analysis of structures. The model is implemented into the special purpose finite element code (*MASA*) and coupled with the nonlocal microcrack interaction approach. In the present paper the numerical results for beam-column connections made of normal and high strength concrete (NSC and HSC) with different amount of reinforcement are presented and discussed.

Key words: Cyclic loading, damage, frames, finite elements, microplane model, reinforced concrete.

1 Introduction

In order to avoid brittle failure and to make the distribution of internal forces possible, any reinforced concrete (RC) structure should fail in a ductile manner. This requirement is specially of a great importance when

the structure is to be exposed to the seismic action i.e. under cyclic loading. The joints between the beams and columns are in RC frame structures particularly important for their ultimate structural resistance as well as for their ductility. They have to transfer high tensile, compressive and shear forces over a relatively small volume of the material. This is strongly pronounced when the beams and columns are provided with relatively high reinforcement ratio. Namely, with more reinforcement the cross-section can transfer higher bending moments and thus generate higher forces that have to be transferred over the joint.

In the past considerable amount of experimental work (Ehsani and Wight, 1986; Leon and Jirsa, 1986; Paulay et al., 1992; Scott, 1992) has been done in order to understand how the joint forces are shared between the concrete and reinforcement during cyclic loading. Currently, a number of research projects for RC frame structures made of high strength concrete (HSC) are on the way. Since HSC has higher strength as well as higher brittleness than the NSC, it is important to know how this influence the performance of the joints in RC frames. Due to the complexity of the problem there is currently no theoretical work which investigates the transfer of forces in the joints under cyclic loading in a three-dimensional stress-strain space. Most of theoretical works are based on one or two-dimensional spatial discretizations which rely on simplified assumptions and therefore do not give a complete picture of that what is actually taking place in the joint during cyclic loading. On the other side, based only on the experiments it is difficult to understand the failure mechanism of joints for different situations that may occur, such as: different loading histories, different concrete qualities, different type and amount of reinforcement. Therefore, there is an obvious need to clarify the failure mechanism in the beam-column joints by theoretical means.

Beam-column joints are exposed to complicated three-dimensional stress-strain states with high compressive, tensile and shear stresses. In the design practice the transfer of forces across the joints is normally calculated by a simple strut and tie models (Schlaich and Schäfer, 1984). According to these models the concrete is mobilized to transfer the compressive forces (diagonal strut) and the reinforcement takes up the tensile forces (tie). To transfer the tensile forces from reinforcement into a compressive concrete struts high bond stresses within the beam-column core should be activated. Since the concrete is a quasibrittle material which under tensile as well as high compressive stresses exhibits relatively brittle behaviour, besides main reinforcement which comes from beams and columns, one needs confinement reinforcement (hoops) which assures the integrity of the joint during alternating cycles of loading and helps in transfer of shear forces. Although the strut and tie model provides an general insight into the joint load transfer mechanism, the way in which are the forces sheared between the diagonal strut and truss mechanism under cyclic loading is difficult to

determinate since it changes due to the progressive increase of damage in the joint.

The main objective of the present study is a theoretical investigation of the beam-column joints under cyclic loading condition using three-dimensional finite element code based on the smeared crack approach. To perform such a study one needs a sophisticated numerical tool which is able to realistically model complicated three-dimensional stress-strain conditions in the joints and do so, not only for monotonic, but also for cyclic loading. The employed material model for concrete should be able to correctly predict behaviour of concrete under triaxial compressive, tensile and shear stresses as well as for their combination. Furthermore, the finite element code must assure objectivity of the analysis with respect to the size and shape of the finite elements. Namely, as soon as damage and cracking phenomena occur the consumption of released structural energy must be mesh independent. Generally, one should use the nonlocal fracture analysis (Ozbolt and Bazant, 1996). However, here considered RC structures provide sufficient main and distributed reinforcement. These reinforcement consume most of the energy released from the structure as a consequence of concrete cracking and assure stable cracking. Therefore, relatively simple scalar type of nonlocality (crack band approach; Bazant and Oh, 1983) used in the study provides sufficient accuracy of the analysis.

2 Material model and finite element discretization

The macroscopical material models are usually formulated by total or incremental formulation between the σ_{ij} and ε_{ij} components of the stress and strain tensor using their invariants (Willam and Warnke, 1974; Ortiz, 1985). Presently there exists no model based on the stress and strain tensor and their invariants that is capable to realistically predict behaviour of concrete under general three-dimensional cyclic loading. In principle the microplane model offers such prediction capability.

In the microplane model (Bazant and Prat, 1988; Ozbolt and Bazant, 1992; Ozbolt et al., 1997) the material properties are characterized separately on planes of various orientations within the material, called microplanes, on which there are only a few stress and strain components and no tensorial invariance requirements need to be observed. The tensorial invariance restrictions are satisfied automatically since the microplanes directly simulate the response on the weak planes in the material (interparticle contact planes, interfaces, planes of microcracks, etc.). The constitutive properties are entirely characterized by a relation between the stress and strain components on each microplane, in both, normal and shear directions. The strain components on the microplane are assumed to be

projections of the total macroscopic strain tensor (damage kinematic constraint approach, Ozbolt et al., 1997). Knowing the stress-strain law for each microplane component, from known microplane strains the macroscopic stiffness and stress tensor are calculated by employing integration of microplane stress components over all microplanes. This integration is performed numerically, based on the virtual work approach. The simplicity of the model is due to the fact that only uniaxial stress-strain laws for each microplane component are required and the macroscopical answer is calculated from the model. It has been shown that the new general nonlocal microplane model for concrete is able to realistically predict behaviour of concrete for any stress-strain history (Ozbolt et al., 1997). The model was coupled with the nonlocal approach (Ozbolt and Bazant, 1996) and implemented into the special purpose FE computer code *MASA* for three-dimensional fracture analysis of concrete and RC structures.

In the present numerical study the concrete is simulated by 3D eight node brick finite elements with eight integration points. The reinforcement is modeled by linear truss elements which are connected to the concrete part of the structure over a common nodes of the brick concrete finite elements. The reinforcement is assumed to have one dimensional ideally elasto-plastic constitutive law. The bond between reinforcement and steel is not explicitly modeled. However, the concrete finite elements around the reinforcing bars are calibrated such that they act as the bond interface elements which approximately simulate bond i.e. the slip is modeled in the smeared sense.

3 Numerical analysis

3.1 Geometry, material properties and the finite element model

The numerical analysis is carried out for beam-column connection that has been tested by Ehsani and Wight, 1986. The geometry of the test specimen with boundary conditions is plotted in Fig. 1a. The experiment studied the influence of the beam and column reinforcement ratio as well as the influence of the slenderness of the beams and columns on the structural response under cyclic loading. The numerical study is carried out only for one geometry (geometry 1B; see Ehsani and Wight, 1986). Fig. 1b shows the 3D finite element mesh employed in the analysis. Note that only one half of the structure was modeled i.e. to reduce the number of finite elements symmetry has been utilized.

Geometrical and material properties for the case studied are summarized in Table 1. As can be seen from Table 1, the beams and columns were in the experiment relatively highly reinforced ($\mu \approx 3\%$). This is for the

ultimate resistance as well as for ductility of the joints rather unfavorable. Namely, beams and columns with high reinforcement ratio at ultimate load generate high forces which must be taken up and transferred over the joint. Furthermore, in such a case the joints accumulate more elastic energy which could be possibly released in an explosive way. The properties of the NSC are taken approximately the same as in the experiment and the compressive and tensile strength of HSC were assumed to be much higher than that of NSC (see Table 1). Figs. 2a,b,c show the constitutive laws for concrete under uniaxial compression and tension as well as the constitutive law for the reinforcement steel.

Table 1. Summary of the material and geometrical properties for:
Concrete - E_c = Young's modulus, ν_c = Poisson ratio, f_c = uniaxial compressive strength, f_t = tensile strength, G_F = fracture energy;
Reinforcement -- f_y = yield stress, $E_s = 200000$ (All units in N and mm)

Concrete	E_c	ν_c	f_c	f_t	G_F	Steel	A_{s1b}	A_{s2b}	ΣA_{sc}	hoops
NSC	25000	0.18	25	2.2	0.1	f_y	331	345	490	437
HSC	40000	0.18	95	4.8	0.2	Area	$3 \phi 22$	$3 \phi 19$	$8 \phi 19$	$\phi 6.5$

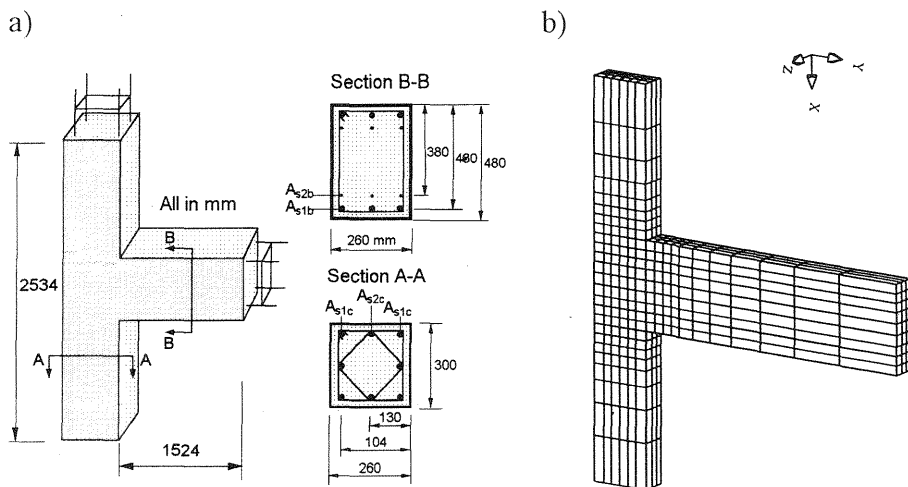


Fig. 1. Beam-column connection: a) geometry and b) finite element model

3.2 Numerical analysis and discussion of the results

The same as in the experiment the structure was first loaded by the compressive column force which corresponds approximately to the compressive stresses $\sigma = 0.1f_c$. The applied cyclic loading followed the displacement controlled schedule at the beam cantilever as shown in

Fig. 2d. The load was first applied in one direction up to the yielding of beam reinforcement (yield displacement) followed by the unloading to zero load and reloading up to approx. 1.5 times of the yield displacement. The structure was then unloaded and loaded in another direction according to scheme plotted in Fig. 2d.

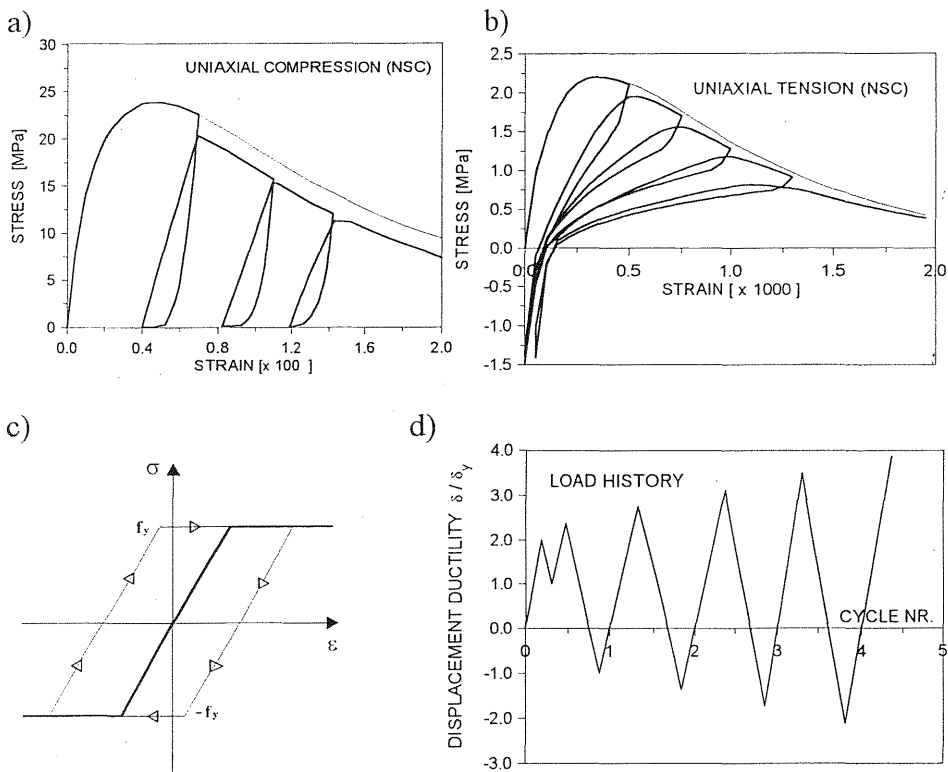


Fig. 2. Constitutive laws and load history: a) uniaxial compression constitutive law for NSC, b) uniaxial tensile constitutive law for NSC, c) constitutive law for reinforcement steel and d) load history

3.2.1 Normal strength concrete

Figs. 3a,b show the calculated and the experimentally measured beam-end load-displacement (L-D) curves, respectively. For comparison, the same figure also shows the calculated L-D curve for monotonic load. The agreement between measured and calculated results is reasonably good. The same as in the experiment, the maximum load in the analysis is reached when the beam reinforcement starts to yield. By subsequently repeated loading the structural resistance as well as its stiffness significantly decrease. The ratio of the maximum load carried by the specimen during

the loading to that of the first cycle is plotted in Fig. 4. The values are calculated as the average of the absolute maximum positive and absolute maximum negative loads carried by the structure during the cycle. As may be seen, the experiment and the analysis show the same tendency i.e. the load-carrying capacity is significantly reduced after the first cycle of loading and it decreases by the increase of the number of loading cycles. Similar as in the experiment, the analysis shows typical "pinching" of the hysteresis loops at midcycle.

There are two reasons for the degradation of the stiffness and reduction of the structural resistance by repeated loading. The first reason is the fact that the flexural cracks near the column and beam surfaces after repeated

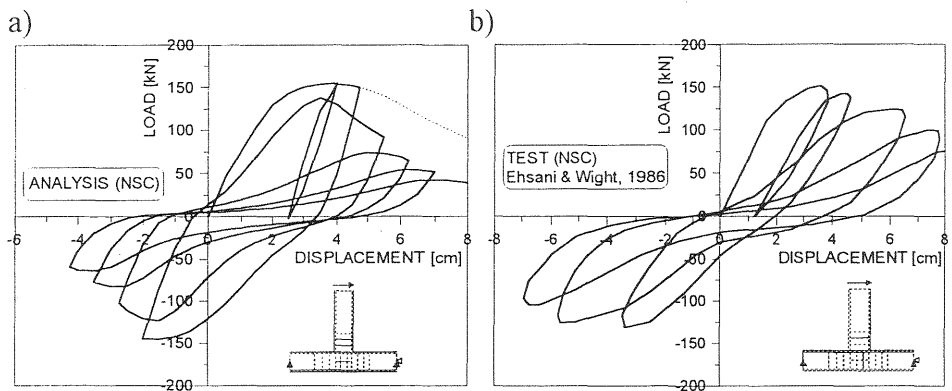


Fig. 3. L-D curves: a) numerical analysis and b) experimental data of Ehsani and Wight (1986)

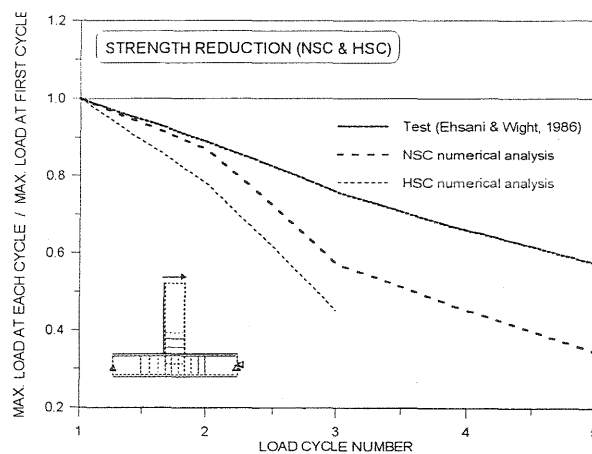


Fig. 4. Calculated (NSC & HSC) and measured (Ehsani and Wight, 1986) decrease of the resistance as a function of the load cycles

loading do not completely close. This is a consequence of concrete damage as demonstrated by Fig. 5. The figure shows concrete damage zones (deformed state) in terms of principal strains at the end of the first (Fig. 5a) and third (Fig. 5b) loading cycle. Damage of the beam and column concrete cover can be seen what reduces compressive stiffness of their cross-sections and, therefore, their peak resistance as well. The fact that the bending cracks do not close after repeated loading confirms also Fig. 6a. The figure shows the variation of the strains (calculated and measured) in the longitudinal beam reinforcement during the cyclic loading. It may be seen that by loading in the opposite direction the reinforcement strains keep the same sign i.e. they are positive (tension).

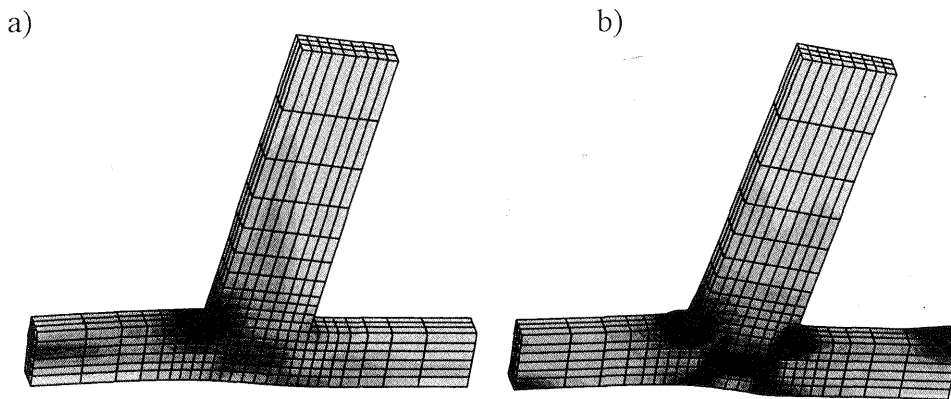


Fig. 5. Localization for damage for NSC (in terms of principal strains) shown on the deformed structure after: a) one loading cycle and b) after three loading cycles

The second reason why the stiffness decreases at each additional cycle of loading is a consequence of accumulated concrete damage in the joint. Fig. 5b clearly shows significant shear damage in the joint reinforcement anchorage zones. Note for cyclic loading typical "X" formed damage zones. The fact that the strains in the vertical hoops of the joint increases when the number of loading cycles increases (see Fig. 7) is also an indicator of the strong concrete damage (expansion) in the joint. Consequently, the bond strength of reinforced bars in the joint decreases what causes slippage of both, column and beam longitudinal reinforcement. This confirms Fig. 6 which shows the strain history (measured and calculated) of the longitudinal column and beam reinforcement. The figure shows that inspite of the substantial increase of displacements by repeated loading the reinforcement strains stay constant or even decrease, what is a clear indication for slippage. Finally, the same as in the experiment, the reason for failure was the pull-out of the beam longitudinal reinforcement.

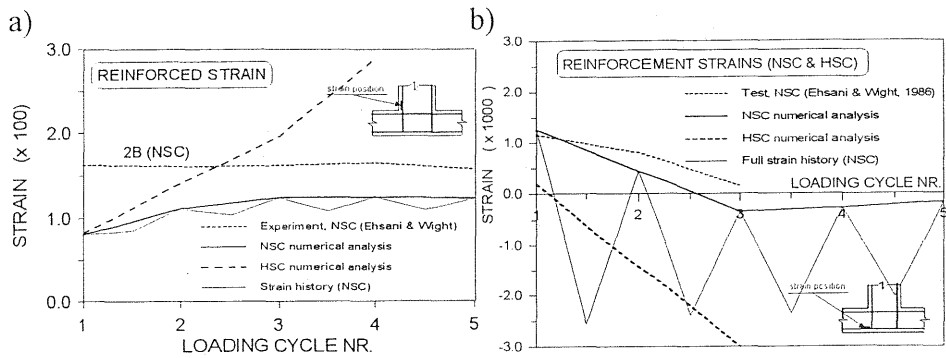


Fig. 6. Measured and calculated distribution of reinforcement strains: a) longitudinal beam reinforcement and b) column reinforcement

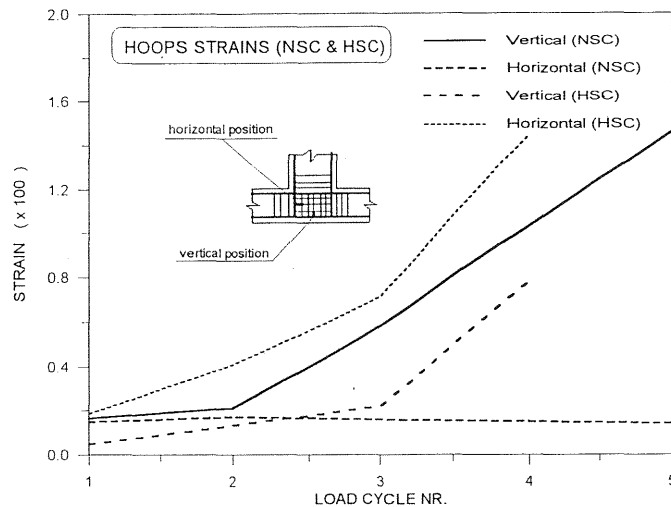


Fig. 7. Calculated distribution of hoops strains

3.2.2 High strength concrete

The same analysis was carried out for HSC. The geometry and the steel reinforcement properties were the same as for NSC except for the concrete properties (see Table 1). Fig. 8 shows the calculated L-D curve. The degradation of the peak resistance with the increase of loading cycles is plotted in Fig. 5. The peak resistance is reached by the yield of beam reinforcement and it is approximately the same as for NSC. The reason is the same reinforcement ratio and relatively small contribution of higher tensile strength of the HSC to the peak resistance.

The calculated reduction of the peak resistance is slightly higher than for the NSC. However, the reduction of the structural stiffness by repeated

loading is much smaller than observed for NSC. Furthermore, although the same cyclic rules as for the NSC have been used, one can not see the typical "pinching" of the hysteresis loops at midcycle. After a number of loading cycles the structure failed not in the joint, as for the NSC, but due to the damage of the beam and column cross-sections.

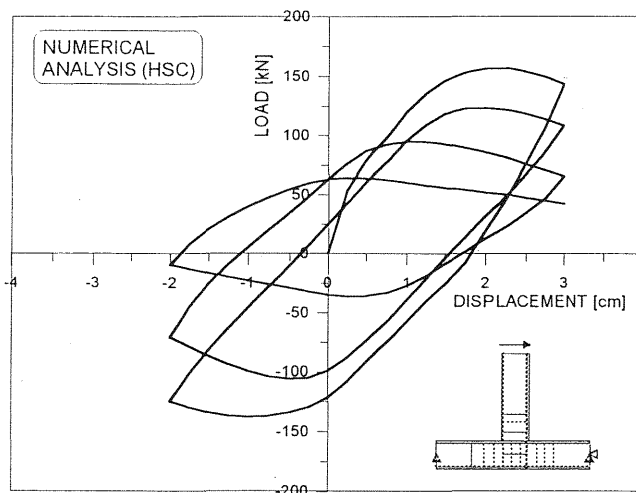


Fig. 8. Calculated L-D curves for HSC

The reason for the reduction of the structural resistance by increase of loading cycles is due to the not completely closed bending cracks as well as due to the damage of the concrete at the beam and column surfaces, the same as observed for NSC. This may be seen in Figs. 9a,b which show the damage zones of the structure in the deformed state after the first and the third loading cycle. As may be seen, the damage zones are localized only at the concrete surface of the beam and column.

The reason why the significant decrease of the stiffness does not take place is caused by the fact that the concrete in the joint was not damaged. This is due to the relative to the concrete strength small stresses in the joint. Consequently, no significant slippage of beam and column reinforcement occurs. Therefore, the stiffness of the structure is mainly controlled by the stiffness of the beam and column cross-sections. This confirms the reinforcement strain histories of the beam and column plotted in Fig. 6. As may be seen the strains increase with increase of the loading cycles, what indicates that no significant damage of the bond takes place. The same is observed for hoops reinforcement (see Fig. 7). Unfortunately, for the present structure type made of HSC no test exists and, therefore, the comparison with test data can not be done.

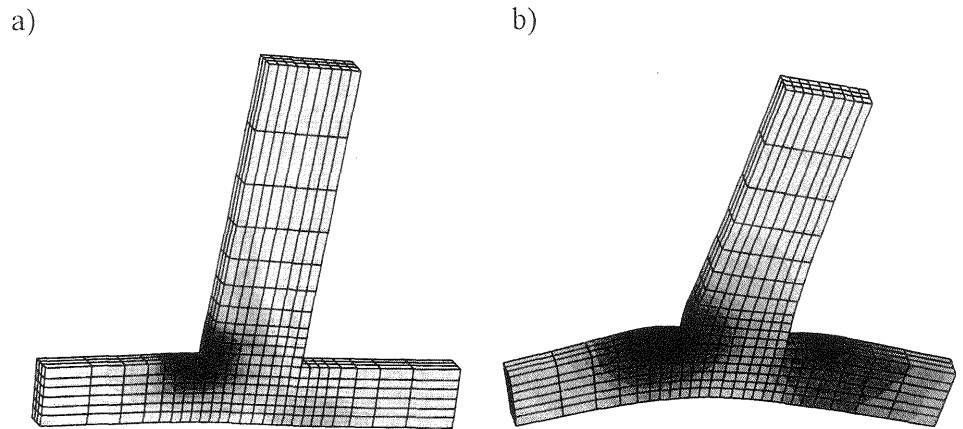


Fig. 9. Localization for damage for HSC (in terms of principal strains) shown on the deformed structure after: a) one loading cycle and b) after three loading cycles

3.2.3 Influence of the longitudinal (main) reinforcement

In the above present numerical results the amount of main beam and column reinforcement and hoops was as specified in Table 1. To investigate the influence of the main reinforcement on the failure mode and resistance of the connection made of NSC the amount of hoops was kept constant and the reinforcement ratio in beam and column was varied from approximately 1 to 5%. The analysis was carried out only for monotonic load.

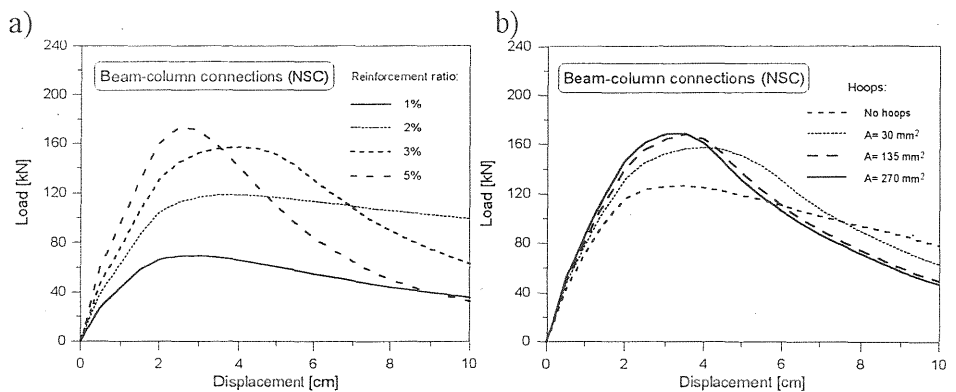


Fig. 10. a) Calculated L-D curves for NSC, connections with different ratio of main reinforcement, b) calculated L-D curves for connections made of NSC with different amount of hoops

Calculated L-D curves are plotted in Fig. 10a. As expected, with increase of the reinforcement ratio the peak load increases and ductility decreases. Structures with smaller reinforcement ratio (1-2%) fail due to the yielding of reinforcement in the column critical cross-section in a ductile manner (see Fig. 11a). On the contrary, structures with higher reinforcement ratio fail in a more brittle manner due to the diagonal shear failure or as a consequence of the pull-out of the beam reinforcement from the joint (see Fig. 11b).

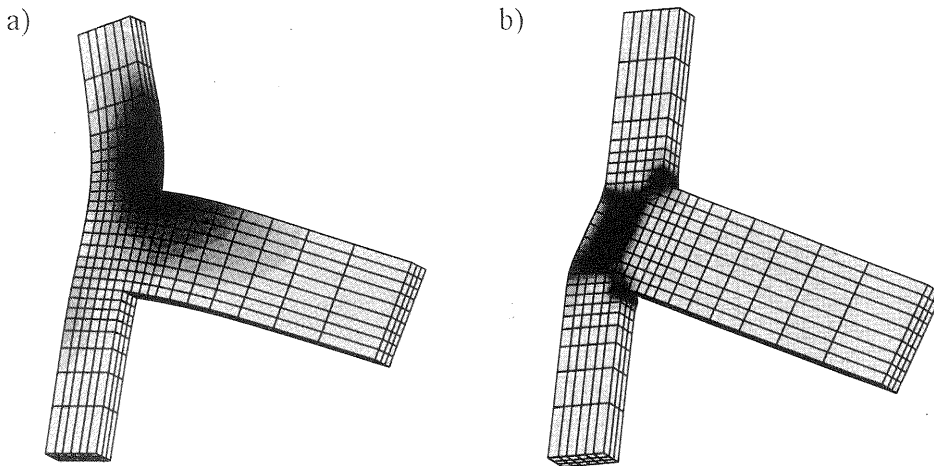


Fig. 11. Localization for damage for NSC connections (principal strains) at peak load for: a) main reinforcement ratio of 1% and b) reinforcement ratio of 5%

3.2.4 Influence of the hoops

To demonstrate the influence of the amount of hoops on the behavior of beam-column connections made of NSC, the main reinforcement in the beams and columns was kept constant (approximately 3%), however, the hoops area was varied. Their spacing was kept constant and it was the same as in the cyclic analysis. The cross section area was varied from 0 to 270 mm² (0, 35-cyclic analysis, 135 and 270 mm²).

Calculated L-D curves are plotted in Fig. 10b. As can be seen, the increase of the hoop area with keeping constant and relatively high main reinforcement ratio in column and beam (approx. 3%) causes an increase of the peak load (see Fig. 10b). The peak resistance of the structure with hoops is max. about 40% higher that the resistance of the same structure without hoops. Obviously, larger amount of hoops means better confinement of the compressive beam zone what increases the lever arm between compression and tension forces of the critical cross-section.

Consequently, for the same tensile force in the reinforcement (yield limit) bending moment increases. Fig. 10b also indicates that the increase of the hoops area leads to a decrease of ductility.

The damage zones for the case without hoops and with hoop area of 270 mm^2 are shown in Fig. 12. Structure without hoops fails in diagonal shear of column cross-section (Fig. 12a) and the structure with high amount of hoops fails due to the pull-out of reinforcement from the beam-column connection (Fig. 12b).

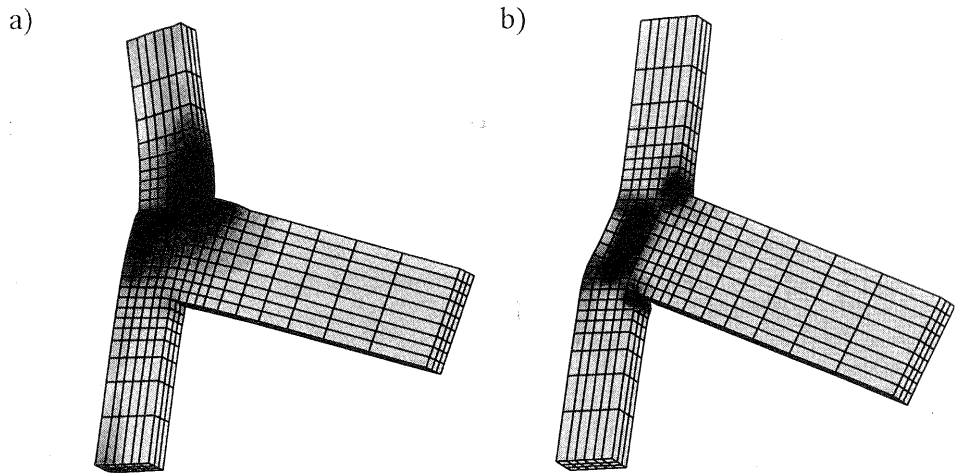


Fig. 12. Localization for damage for NSC connections (principal strains) at peak load for: a) no hoops and b) hoops area = 270 mm^2

4 Conclusions

- For the present example the NSC beam-column connection indicated a significant decrease of the peak resistance with increasing loading cycles. Furthermore, typical "pinching" was observed, mainly caused by the significant concrete damage in the joint. The structure failed due to the failure of the bond resistance in the joint.
- The beam-column connection made of HSC also exhibit relatively strong reduction of the resistance with increase of the number of loading cycles. However, the reduction of the stiffness at the midcycle was not observed. The reason are smaller stresses relatively to the concrete strength in the joint which makes anchorage of the longitudinal beam and column reinforcement effective. The failure of the structure was fully controlled by the stiffness of the beam or column cross-section.

- The behavior of joints under monotonic loading depends on the amount of the main beam and column reinforcement as well as on the amount of the hoops. At constant hoops, increase of the main reinforcement leads to the increase of the peak load and decrease of ductility. Similar effect was observed when the main reinforcement was kept constant and the amount of hoops was increased.
- Three-dimensional analysis based on the general microplane material model for concrete is able to realistically predict the behaviour of beam-column connections under cyclic and monotonic loading. The numerical results for the present example qualitatively and quantitatively agree well with the experimental observations.

5 References

- Bazant, Z.P. and Oh, (1983) Crack band theory for fracture of concrete, **Materials and Structures**, RILEM, 93, 16, 155-177.
- Bazant, Z.P. and Prat, P.C. (1988) Microplane model for brittle-plastic material - parts I and II, **JEM-ASCE**, 114, 10, 1672-1702.
- Ehsani, M.R. and Wight, J.K. (1986) Exterior reinforced concrete beam-column connections subjected to earthquake type loading, **Journal of ACI**, 82, 43, 492-499.
- Leon, R. and Jirsa, R.H. (1986) Bi-directional loading of RC beam / column joints, **EERI Earthquake Spectra**, 2, 3, 537-564.
- Ortiz, M.A. (1985) A constitutive theory for the inelastic behaviour of concrete, **Mech. and Matls**, 4, 67-93.
- Ozbolt, J. and Bazant, Z. P. (1992) Microplane model for cyclic triaxial behaviour of concrete, **JEM-ASCE**, 118, 7, 1365-1386.
- Ozbolt, J. and Bazant, Z.P. (1996) Numerical smeared fracture analysis: Nonlocal microcrack interaction approach, **IJNME**, 39, 4, 635-661.
- Ozbolt, J., Li, Y. and Kozar, I. (1997) Microplane Model for Concrete, submitted for publication in **IJSS**.
- Paulay, T., Park, R. and Priestley, M.J.N. (1978) Reinforced concrete beam / column joints under seismic action, **Journal of ACI**, 75, 11, 585-593.
- Schlaich, J. and Schäfer, K. (1984) Konstruktionen im Stahlbeton, **Beton-Kalender**.
- Scott, R.H. (1992) The effect of detailing on reinforced concrete beam-column connection behaviour, **The Struct. Eng.**, 70(18), 318-324.
- Taylor, G.I. (1938) Plastic strain in metals, **JIM**, 62, 307-324.
- Willam, K.J. and Warnke, E.P. (1974) Constitutive model for triaxial behaviour of concrete, Seminar on Concrete Structures Subjected to Triaxial Stresses, **Int. Assoc. of Bridge and Struct. Engrg. Conf.**, Bergamo, Italy.